

ELECTRICAL AND MAGNETORESISTIVE PROPERTIES OF THE Ag/La_{2/3}Sr_{1/3}MnO₃ POINT-PROBE CONTACTS

I. Černiukė^a, B. Vengalis^a, A. Steikūnienė^a, G. Grigaliūnaitė-Vonsevičienė^b,
and A.K. Oginskis^a

^aCenter for Physical Sciences and Technology, A. Goštauto 11, LT-01108 Vilnius, Lithuania

^bVilnius Gediminas Technical University, Saulėtekio 11, LT-10223 Vilnius, Lithuania

E-mail: veng@pfi.lt

Received 1 October 2014; revised 13 October 2014; accepted 10 December 2014

We report electrical and magnetoresistive properties of Ag point-probe contacts formed by attaching the bent Ag wire ($\varnothing = 0.25$ mm) to the top of the La_{2/3}Sr_{1/3}MnO₃ (LSMO) thin film magnetron sputtered at 800 °C on MgO(100) single crystal substrates. Significant contact magnetoresistance values (up to 13% at $T = 295$ K and $\mu_0 H = 0.73$ T) have been measured for the Ag/LSMO junctions by applying a 3 point-probe method. The origin of both temperature-dependent resistance and magnetoresistance of the Ag/LSMO contacts has been explained taking into account the dominating role of spreading resistance. It was found that keeping of the films in air for 1 month as well as ultrathin overlayers ($d \sim 3$ – 5 nm) of the highly resistive multiferroic BiFeO₃ magnetron sputtered onto the manganite film resulted in a significant increase of contact resistance and reduced magnetoresistance values.

Keywords: manganite films, magnetoresistance, 3 point-probe method, contact resistance, spreading resistance

PACS: 73.40.Cg, 73.43.Qt, 75.47.-m

1. Introduction

Lanthanum manganites referred to by the general formula La_{1-x}A_xMnO₃ (A = Ca, Sr, Ba) demonstrate a variety of interrelated structural, electrical and magnetic properties. The member compounds with $x = 0.33$ provide great interest due to the observed carrier-driven paramagnetic (PM) to ferromagnetic (FM) transition at the Curie temperature (T_C), the so-called “colossal” magnetoresistance (MR) and presence of spin-polarized carriers at $T < T_C$. La_{0.67}Sr_{0.33}MnO₃ (LSMO) demonstrating the highest T_C value (350 K) among other member compounds [1] provides increasing interest for room temperature applications. Thin LSMO films are promising for the fabrication of magnetic field sensors, nonvolatile memory devices and other spintronics devices [2–6].

Heterojunctions formed between manganite thin films and typical semiconductors as Si and Nb-doped SrTiO₃ attract interest due to magnetic field-dependent rectifying I – U characteristics and photovoltaic effect [5–9]. Similar heterojunctions formed between conventional metals such as Ag, Au and hole-doped manganites have been investigated due mainly to the electric field-induced resistive switching phenomenon and resistive memory applications [10, 11]. However, only

few data has been reported till now on interface resistance [12–14] although metallic contacts are widely used for various spintronics devices. Furthermore, up to date there is a lack of information on magnetoresistive properties of the metal/manganite junctions.

Investigation of the electrical transport across interfaces between manganite thin films and metals (Ag, Au, Nb, Pd, Al...) shows that the corresponding interface resistance referred hereafter as contact resistance (R_c) can vary in wide ranges. It depends mainly on the chemical reactivity of metal resulting in oxygen loss at the manganite film interface and possible formation of highly resistive interlayers [13, 15]. Importance of the chemical activity of the manganite film surface with regard to air and various solvents used during processing has been pointed out additionally [14].

Low value of contact resistivity ($\rho_c = R_c S$, here S is the contact area) of about 10^{-5} Ωcm^2 (at $T = 4.2$ K) has been measured for the Au/La_{0.34}Sr_{0.66}MnO₃ interface (with $S = 20 \times 20$ μm^2) patterned in a cross stripe geometry [14]. Similar ρ_c values, i. e. of about 10^{-5} Ωcm^2 and 10^{-6} Ωcm^2 (at $T = 300$ K), have been measured, respectively, for the Au/La_{0.70}Ca_{0.30}MnO₃ and Ag/La_{0.70}Ca_{0.30}MnO₃ interfaces ion beam patterned into Kelvin bridge device structures ($S = 5 \times 5$ μm^2) [15]. It is important to note, however, that temperature

dependences of contact resistance of the device structures with patterned planar Ag and Au electrodes show distinctly different behavior when compared to the corresponding film resistance versus temperature dependences. The presence of highly resistive oxide material with reduced oxygen content occurring at the metal/manganite interface during processing has been pointed out to explain anomalous temperature-dependent electrical transport across the interfaces.

To estimate contact resistance of the interface formed between a conventional nonreactive metal (Ag) and LSMO thin film and to investigate magnetoresistance of the Ag/LSMO contact, here in this work we concentrated on a 3 point-probe method (see the inset to Fig. 3). To reduce influence of a possible interfacial layer that can be formed during processing at the metal/manganite interface [14, 15], in this work the central electrode was formed directly by attaching the bent Ag wire onto the LSMO film. Major attention was focused to investigate the influence of temperature and applied magnetic field on both resistance and magnetoresistance of the Ag/LSMO junction and to elucidate the origin of magnetoresistance for the prepared Ag-probe contacts.

2. Experiments

The LSMO films were grown *in situ* at 800 °C on cleaved (100) faces of MgO crystal by magnetron sputtering of the disk-shaped ceramic $\text{La}_{0.67}\text{Sr}_{0.33}\text{MnO}_3$ target ($\varnothing = 25$ mm) in Ar-O₂ mixtures with the molar ratio (1:1) and partial oxygen pressure P_{O_2} of about 15 Pa. The substrate used for film deposition was mounted in the “off-axis” position at a distance of about 50–60 mm from the target plane. Thickness of the films after 3 h deposition (measured by a DEK-TAK profilometer) varied from about 200 to 250 nm. After deposition, the films were cooled down slowly to a room temperature under oxygen gas pressure of about 5×10^4 Pa to ensure oxygen stoichiometry in the whole film material.

In order to modify the LSMO film surface, some part of the film was coated by ultrathin overlayers of highly resistive multiferroic BiFeO₃ compound. The BFO layers were prepared onto the LSMO films *in situ* at 750 °C by radio frequency (rf) magnetron sputtering of the ceramic BiFeO₃ target as it was described earlier [16]. Averaged thickness of the BFO overlayer ($d \sim 3\text{--}5$ nm) was estimated from the deposition duration.

A crystalline structure of the grown LSMO films was analysed by X-ray diffraction (XRD) in Θ -2 Θ geometry using CuK $_{\alpha}$ radiation ($\lambda = 0.15406$ nm) while

their surface roughness was studied by atomic force microscopy (AFM).

Electrical resistance of the LSMO films was measured in the temperature range 80–350 K by a conventional 4-probe method using DC current $I = 0.1$ mA. Negative magnetoresistance of the prepared films, MR_{LSMO} , defined as $\Delta R/R_0 = [R_{\text{LSMO}}(H=0) - R_{\text{LSMO}}(H)]/R_{\text{LSMO}}(H=0)$, was estimated by applying magnetic field ($\mu_0 H = 0\text{--}0.73$ T), either parallel (H_{\parallel}) or perpendicular (H_{\perp}) to the film plane.

Contact resistance ($R_{\text{Ag/LSMO}}$) and the corresponding magnetoresistance of the Ag/LSMO contacts ($MR_{\text{Ag/LSMO}}$) were measured by applying a 3 point-probe method, i. e. by passing current $I \leq 1$ mA between contacts 1 and 2 and measuring voltage between 2 and 3 as shown in the inset to Fig. 3.

The bent Ag wire probe with a diameter of 0.25 mm pressed mechanically to the manganite film surface was used as a testing electrode. The Ag probe was fixed to a special strip limiting probe motion along one direction (perpendicularly to the film plane). A special design of a sample/probe holder has been elaborated either to vary the applied pressing force F gradually in the range 0–2.0 N or to keep it fixed during long time independently on the temperature and the applied magnetic field.

The Ag/LSMO contacts formed on the top surface of just prepared LSMO film, a similar film kept after deposition during 1 month in air atmosphere and that buffered by an ultrathin highly resistive BiFeO₃ (BFO) overlayer were investigated for a comparison.

3. Characterization of the $\text{La}_{0.67}\text{Sr}_{0.33}\text{MnO}_3$ films

The Θ -2 Θ X-ray diffraction scan of the LSMO/MgO(100) film formed at 800 °C is displayed in Fig. 1. Clearly defined XRD lines of the (00 l) family ($l = 1, 2, \dots$) seen in the figure certify the growth of single phase highly textured material with [100]-axis aligned normal to the film plane. The off-plane lattice constant of a pseudocubic unit cell, $a_{\text{LSMO}} = 0.3885$ nm, has been estimated for the LSMO film in good accordance to recently published data [11, 17].

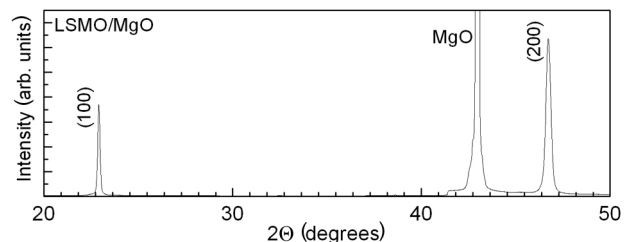


Fig. 1. Θ -2 Θ XRD patterns of the LSMO/MgO(100) film grown by magnetron sputtering at 800 °C.

A typical AFM surface image of the LSMO film is displayed in Fig. 2. The averaged surface roughness of about 5.5 nm has been estimated for the prepared LSMO/MgO film.

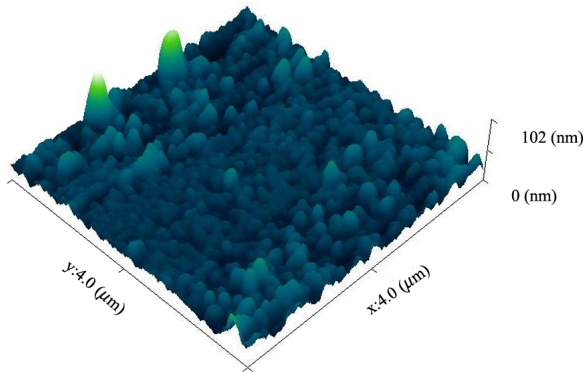


Fig. 2. A typical AFM surface image of the LSMO film grown on the MgO(100) substrate at 800 °C.

4. Results of electrical measurements and discussion

In order to get the most reproducible results and to avoid possible probe-induced damage of the manganite film surface and to find an optimal load force for the Ag probe, series of contact resistance measurements were performed by a 3 point-probe method.

Figure 3 shows a typical variation of contact resistance ($R_{\text{Ag/LSMO}}$) measured at $T = 295$ K by applying

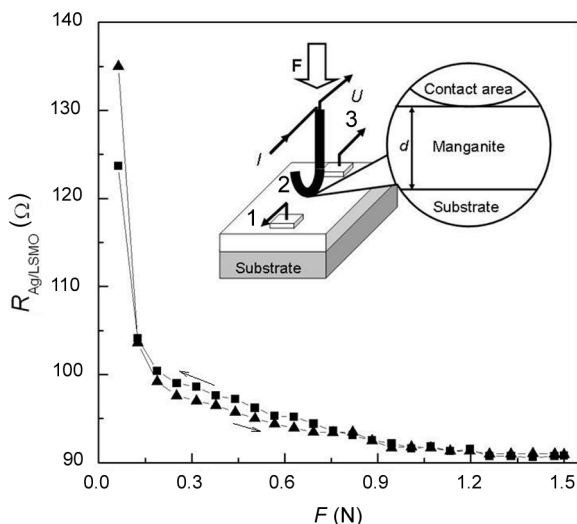


Fig. 3. Contact resistance of the Ag probe electrode measured at 295 K by a 3 point-probe method with load force, F , increasing and decreasing gradually in the range 0–1.5 N. A schematic drawing of the 3 point-probe measurement circuit is displayed in the inset.

a 3-probe method with load force, F , increasing and decreasing gradually in the range 0–1.5 N. Before the measurements, the load force of 1.5 N was applied to the Ag probe contact and kept during 1 h to achieve long-term stability of the contact. Following Fig. 3, one can notice a sharp drop of the measured $R_{\text{Ag/LSMO}}$ values with load force increasing in the range 0–0.2 N, gradual decrease of $R_{\text{Ag/LSMO}}$ values with following F increase up to about 1.2 N and negligible interface resistance variation for $F = (1.2\text{--}1.5)$ N. It is worth noting that electrical behaviour of the Ag probe contacts is unstable at the lowest load force values ($F < 0.2$ N). The observed gradual contact resistance decrease with F increasing in the intermediate region may be associated with a certain increase of the active contact area due, probably, to elastic deformation either of the Ag-probe electrode or the LSMO film.

The most stable electrical properties of the Ag probe contacts with linear current-voltage relations and reproducible contact resistance measurements have been realised in this work by applying $F = (1.2\text{--}1.5)$ N. All following measurements of both contact resistance and magnetoresistance have been performed in this work at the fixed load force $F \cong 1.5$ N. Contact resistance of the as-prepared Ag-probe contacts varied statistically within about $\pm 15\%$ from the average value by changing the position of the contact on the film surface. The average diameter of the contact of about 3–5 μm has been estimated in this work following the observed AFM image of a track with a slightly damaged film surface caused by the Ag probe ($F = 1.5$ N) moving along the film.

In Fig. 4(a) we show the resistance of the LSMO film, R_{LSMO} , and the contact resistance, $R_{\text{Ag/LSMO}}$, both measured in the absence of magnetic field (solid lines) and at magnetic field ($\mu_0 H_{\parallel} = 0.73$ T) directed parallel to the film surface (dotted lines). The R_{LSMO} and $R_{\text{Ag/LSMO}}$ versus temperature plots displayed in Fig. 4(a) are normalized to the corresponding maximal zero field resistance values for a comparison.

The observed decrease of film resistance (by a factor of 30) with T decreasing from T_p down to 80 K is characteristic of high crystalline quality (epitaxial) LSMO films exhibiting the characteristic paramagnetic to ferromagnetic (PM-FM) transition at $T \approx T_p$. A shift of T_p values to lower temperatures for LSMO and other manganite films is usually associated with lowered carrier density in the film material. From this point of view it is important to note similar resistance peak temperatures (at $T \cong 315$ K) seen in Fig. 4(a) from the $R_{\text{Ag/LSMO}}(T)$ and $R_{\text{LSMO}}(T)$ plots and a gradual decrease of both R_{LSMO} and $R_{\text{Ag/LSMO}}$ values with T decreasing from the characteristic resistance peak temperature T_p . Thus, in contrast to earlier observations [14, 15], one can conclude that carrier density in the vicinity of the

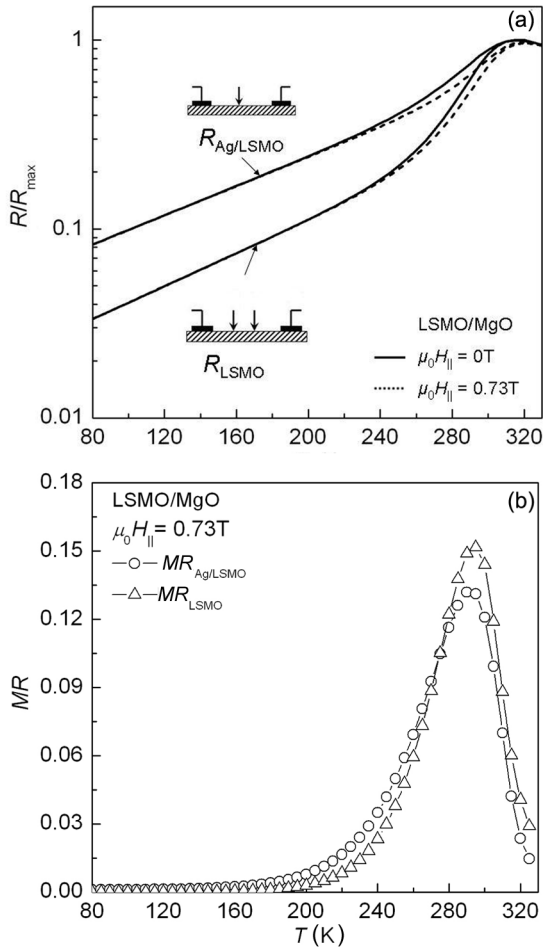


Fig. 4. Resistance of the LSMO film and that of the Ag/LSMO contact normalized to maximal zero field values (a), the corresponding film (MR_{LSMO}) and contact magnetoresistance ($MR_{\text{Ag/LSMO}}$) (b) have been measured under magnetic field $\mu_0 H_{\parallel} = 0.73$ T directed parallel to the film plane.

Ag/LSMO interface (being responsible for contact resistance) is similar to that in the film (far from the interface). Nevertheless, following Fig. 4(a) we note a reduced decrease of contact resistance (by a factor of about 12) with T lowering from T_p down to 80 K in comparison to variation of $R_{\text{LSMO}}(T)$ (by a factor of about 30) in the same temperature range. This difference may be associated with a certain influence of a possible ultrathin surface layer with reduced carrier density and increased resistivity at low temperatures existing naturally on manganite films [18].

Magnetoresistance versus temperature measured for the LSMO film (MR_{LSMO}) and for the Ag/LSMO contact ($MR_{\text{Ag/LSMO}}$) at magnetic field $\mu_0 H_{\parallel} = 0.73$ T directed parallel to the film plane are displayed in Fig. 4(b). A slightly lower maximal value of contact magnetoresistance, $MR_{\text{Ag/LSMO}}$, of about 13% com-

pared to the maximal film magnetoresistance ($\sim 15\%$) may be a result of a possible ultrathin surface layer with lowered carrier density and reduced magnetic properties that is a common feature of most manganite films. Rather low MR_{LSMO} and $MR_{\text{Ag/LSMO}}$ values seen from Fig. 4(b) at $T < 100$ K certify a negligible role of intergrain boundaries on both magnetoresistance of the film and that of the Ag/LSMO junction.

To better understand formation of an electrical contact between the Ag probe electrode and the LSMO film and to reveal the origin of contact magnetoresistance, three kinds of Ag/LSMO contacts were investigated for a comparison. The first group of contacts was formed on the top surface of just prepared LSMO film, the second group was formed on a similar film kept after deposition during 1 month in air atmosphere and the third group of contacts was formed on the LSMO film buffered just after preparation by an ultrathin highly resistive BiFeO_3 (BFO) overlayer with a thickness of about 3–5 nm. Typical contact resistance values measured at room temperature for the contacts on just prepared LSMO films ranged from about 90 to 120 Ω while slightly higher $R_{\text{Ag/LSMO}}$ values (up to about 200 Ω) have been measured for a similar contact formed on the same film kept after deposition in air atmosphere during 1 month. No changes in film resistance (R_{LSMO}) and in the corresponding resistance peak temperature (T_p) values have been indicated either due to keeping of the films in air during 1 month or sputtering of the BFO overlayers.

In Fig. 5(a, b) we show the junction resistance of various point-like Ag contacts measured at $T = 295$ K as a function of magnetic field directed parallel (H_{\parallel}) and normal (H_{\perp}) to the film plane, respectively. All the dependences displayed in Fig. 5(a, b) are normalized to the corresponding zero field values for a comparison.

All the prepared Ag/LSMO junctions demonstrated reduced contact resistance variation with magnetic field (see curves 2, 2' and 3 in Fig. 5(a, b)) compared to that of the LSMO film (curves 1). It can be seen from Fig. 5(a, b) that the LSMO film kept for a long time in air atmosphere demonstrates slightly lowered contact magnetoresistance (curves 2') compared to similar contacts formed onto just prepared LSMO film (see curves 2) while the presence of an ultrathin BFO overlayer resulted in a significantly reduced contact magnetoresistance (curves 3).

Nonlinear $R_{\text{LSMO}}(H)$ and $R_{\text{Ag/LSMO}}(H)$ dependences and their significant anisotropy at low magnetic fields ($\mu_0 H_{\parallel}, \mu_0 H_{\perp} < 0.2$ T) (see the corresponding plots in Figs. 5(a, b)) can be explained within a common model taking into account importance of internal magnetic field (magnetisation) on both film resistance and

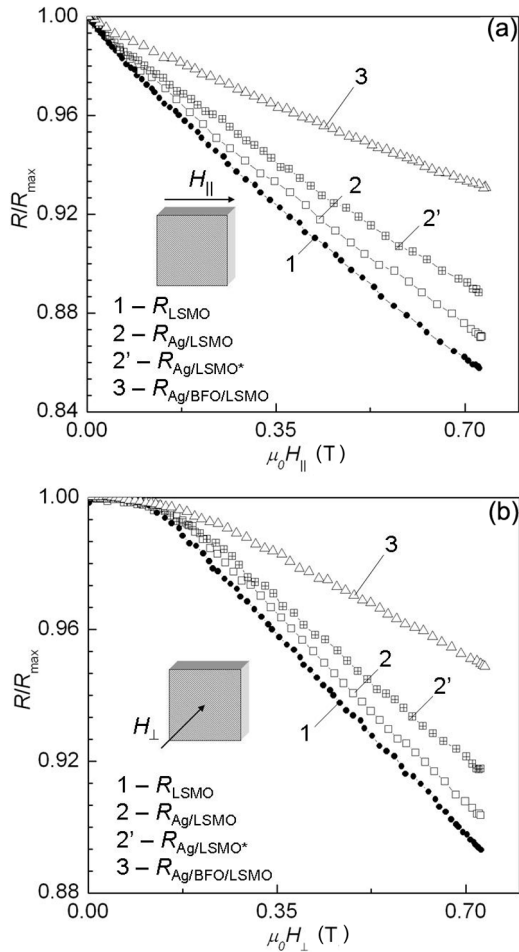


Fig. 5. In-plane LSMO film resistance (1) and contact resistance of the Ag/LSMO (2), Ag/LSMO* (2') and Ag/BFO/LSMO (3) junctions measured at $T = 295$ K and normalized to the corresponding zero field values. Magnetic field directed parallel (H_{\parallel}) (a) and normal (H_{\perp}) to the film plane (b).

contact resistance and assuming different magnetization conditions with H applying parallel and perpendicular to the film plane. Certainly, an easy magnetization axis of the ferromagnetic film including manganites is usually parallel to the film plane [19].

Figure 6 shows a clear correlation between sets of contact resistance and contact magnetoresistance values ($\mu_0 H_{\parallel} = 0.73$ T) measured at $T = 295$ K for three kinds (Ag/LSMO, Ag/LSMO* and Ag/BFO/LSMO) of contacts. The junctions corresponding to each group have been formed under identical conditions at different locations of the same films.

A relatively small variation of both junction resistance and magnetoresistance values has been indicated for the contacts formed on the LSMO film just after film preparation. Keeping the samples in ambient air for 1 month resulted in a slight increase of R_c and decrease of MR_c values due, probably, to an additional loss

of oxygen from the LSMO surface and development of a highly resistive surface layer. At the same time, the presence of a highly resistive ultrathin BFO layer resulted in a significant increase of contact resistance and decrease of contact magnetoresistance values. Variation of both R_c and MR_c values in the last case can be explained assuming a possible nonuniform thickness of the highly resistive overlying BFO film being of key importance for tunnelling of carriers via the ultrathin BFO interlayer.

We are turning now to discuss the origin of magnetoresistance of the contact formed between the Ag wire probe and the LSMO film. It can be seen from Fig. 6 that the highest MR_c values measured at room temperature have been indicated for the contacts formed onto the surface of just prepared LSMO film.

Due to rather low contact resistivity values ($\rho_c \sim 10^{-5} \Omega\text{cm}^2$) estimated in this work at $T = 295$ K in the case of uniform current flow via the effective junction area $S = 10 \mu\text{m}^2$, linear current–voltage relations measured for the junctions in the whole temperature range and high carrier density ($\sim 10^{21} \text{cm}^{-3}$) in manganite we avoid importance of possible Schottky barrier formation on both resistance and magnetoresistance of the Ag/LSMO junction. Taking into account relatively large contact resistance values ($R_c \sim 100 \Omega$) in the case of a small interface area, we stress importance of spreading resistance (R_{spr}) [20] for both resistance and magnetoresistance of the Ag/LSMO contacts.

The spreading resistance is known to arise from spreading of current flow lines from a metallic

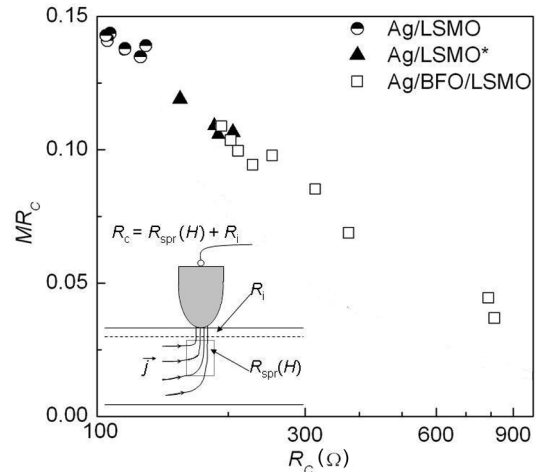


Fig. 6. Contact magnetoresistance (MR_c) ($\mu_0 H_{\parallel} = 0.73$ T) versus contact resistance (R_c) measured at $T = 295$ K for the Ag/LSMO, Ag/LSMO* and Ag/BFO/LSMO junctions. Distribution of current lines in the LSMO film below the Ag probe is shown schematically in the inset.

electrode toward the bulk of a conductor. In the case of a round metallic electrode with resistivity ρ_M , radius a and contact area $S_c^* = \pi a^2$ prepared on the top of the bulk conductor with resistivity $\rho \ll \rho_M$ it can be estimated from the equation [20]:

$$R_{\text{spr}} = \rho \frac{l^*}{S_c^*} = \frac{\rho}{4a}, \quad (1)$$

where $l^* = \pi a/4$ is the effective current-carrying channel length.

Relatively low R_{spr} values (of about 1–2 Ω) can be estimated from Eq. (1) for a round Ag probe with a diameter of 3–5 μm when formed on a bulk LSMO crystal. However, one can expect that R_{spr} values should be significantly higher for similar contacts formed on thin films with the thickness $d \ll a$. Certainly, in the case of the contact formed on a thin film, spreading resistance arises from sharp bending of current lines in the vicinity of the top electrode (see inset in Fig. 6) and the effective cross section of the material current flow lines concentrated below the contact should be limited by film thickness. Further, taking into account a relatively rough LSMO surface (see AFM image in Fig. 2) one can expect that current lines crossing the interface may be distributed nonuniformly. So R_{spr} could be increased additionally taking into account a reduced effective area of the interface.

Taking into account the dominating role of spreading resistance for the Ag/LSMO probe contacts demonstrating the lowest contact resistance and the highest magnetoresistance values as well a clear correlation between R_c and MR_c values for the contacts formed on the LSMO films kept for a long time in ambient air and those buffered by highly resistive BFO overlayers, we further assume that in a general case contact resistance for small area contacts might be considered consisting of two parts according to Eq. (2):

$$R_{\text{Ag/LSMO}}(H) = R_{\text{spr}}(H) + R_i, \quad (2)$$

where $R_{\text{spr}}(H)$ is magnetic field-dependent spreading resistance that is a common feature of small interface area electrodes [20] and R_i is temperature-dependent additional resistance that can be related either to a possible highly resistive surface layer (with reduced oxygen content, lowered carrier density and reduced magnetic order parameter [18]) or an additionally evaporated overlying film of nonmagnetic material.

Summarizing, we conclude that the contact resistance ($R_{\text{Ag/LSMO}}$) and magnetoresistance ($MR_{\text{Ag/LSMO}}$) of the point-like contact formed by attaching the Ag wire to the LSMO film surface have been measured in a wide temperature range ($T = 350\text{--}80\text{ K}$) by applying a 3 point-probe method. The highest magnetoresis-

tance values of the Ag/LSMO interface up to 13% (at $T = 295\text{ K}$) have been measured by applying magnetic field ($\mu_0 H = 0.73\text{ T}$) parallel to the film surface.

It was found in this work that highly resistive surface layers appearing on the LSMO film surface due either to long-term exposition of the films in air or evaporation of highly resistive ultrathin BFO overlayers result in the increase of contacts resistance, $R_{\text{Ag/LSMO}}$, while magnetoresistive properties of the contacts are defined mainly by spreading resistance.

References

- [1] M. Navasery, S.A. Halim, N. Soltani, G. Bahmanrokh, A. Dehzangi, M. Erfani, A. Kamalianfar, S.K. Chen, and K.Y. Pan, High Curie temperature for $\text{La}_{5/8}\text{Sr}_{3/8}\text{MnO}_3$ thin films prepared by pulsed laser deposition on glass substrates, *Int. J. Electrochem. Sci.* **8**, 467–476 (2013).
- [2] D. Hrabovsky, G. Herranz, K. Postava, I.C. Infante, F. Sánchez, and J. Fontcuberta, Optical sensing of magnetic field based on magnetorefractive effect in manganites, in: *Proceedings of SPIE 7356*, Optical Sensors 2009, 73560R (May 18, 2009), <http://dx.doi.org/10.1117/12.820758>
- [3] P. Stoliar, P. Levy, M.J. Sanchez, A.G. Leyva, C.A. Albornoz, F. Gomez-Marlasca, A. Zanini, C. Toro Salazar, N. Ghenzi, and M.J. Rozenberg, Non-volatile multilevel resistive switching memory cell: A transition metal oxide-based circuit, arXiv:1310.3613v1 [cond-mat.other] (2013).
- [4] L. Granja, L.E. Hueso, P. Levy, and N.D. Mathur, Exploiting phase separation in monolithic $\text{La}_{0.6}\text{Ca}_{0.4}\text{MnO}_3$ devices, *Appl. Phys. Lett.* **103**, 062404 (2013), <http://dx.doi.org/10.1063/1.4818314>
- [5] S.S. Zhao, H. Ni, K. Zhao, S.Q. Zhao, Y.C. Kong, and H.K. Wong, High-sensitivity photovoltaic responses in manganite-based heterojunctions on Si substrates for weak light detection, *Appl. Opt.* **50**(17), 2666–2670 (2011), <http://dx.doi.org/10.1364/AO.50.002666>
- [6] Z.J. Yue, K. Zhao, H. Ni, S.Q. Zhao, Y.C. Kong, H.K. Wong, and A.J. Wang, Photo-induced magnetoresistance enhancement in manganite heterojunction at room temperature, *J. Phys. D* **44**, 095103 (2011), <http://dx.doi.org/10.1088/0022-3727/44/9/095103>
- [7] W.M. Lu, J.R. Sun, D.J. Wang, Y.W. Xie, S. Liang, Y.Z. Chen, and B.G. Shen, Bias-dependent rectifying properties of n-n manganite heterojunctions $\text{La}_{1-x}\text{Ca}_x\text{MnO}_3/\text{SrTiO}_3:\text{Nb}$ ($x = 0.65\text{--}1$), *Appl. Phys. Lett.* **93**, 212502 (2008), <http://dx.doi.org/10.1063/1.3021399>
- [8] S. Zhao, K. Zhao, H. Ni, W. Xiang, S. Zhao, Y.-C. Kong, and H.-K. Wong, Manganite heterojunction photodetectors for femtosecond pulse laser measurements, *Opt. Laser Technol.* **44**,

- 1758–1761 (2012), <http://dx.doi.org/10.1016/j.optlastec.2012.02.006>
- [9] Z. Li, M. Bosman, Z. Yang, P. Ren, L. Wang, L. Cao, X. Yu, C. Ke, M.B.H. Breese, A. Ruydy, W. Zhu, Z. Dong, and Y.L. Foo, Interface and surface cation stoichiometry modified by oxygen vacancies in epitaxial manganite films, *Adv. Funct. Mater.* **22**(20), 4312–4321 (2012), <http://dx.doi.org/10.1002/adfm.201200143>
- [10] N. Ghenzi, M.J. Sanchez, F. Gomez-Marlasca, P. Levy, and M.J. Rozenberg, Hysteresis switching loops in Ag-manganite memristive interfaces, *J. Appl. Phys.* **107**, 093719 (2010), <http://dx.doi.org/10.1063/1.3372617>
- [11] T. Yokota, S. Murata, and M. Gomi, Electric field-induced magnetic changes in $\text{La}_{0.7}\text{Sr}_{0.3}\text{MnO}_3$ thin film using electric field-induced resistance phenomenon, *Appl. Phys. Lett.* **102**, 152404 (2013), <http://dx.doi.org/10.1063/1.4802483>
- [12] LI. Abad, B. Martínez, and LI. Balcells, Surface behavior of LCMO epitaxial thin films, *Appl. Phys. Lett.* **87**, 212502 (2005) <http://dx.doi.org/10.1063/1.122261>.
- [13] A. Plecenik, K. Frohlich, J.P. Espinos, J.P. Holgado, H. Halabica, M. Pripko, and A. Gilabert, Degradation of LaMnO_{3-y} surface layer in LaMnO_{3-y} /metal interface, *Appl. Phys. Lett.* **81**(5), 859–861 (2002), <http://dx.doi.org/10.1063/1.1497439>.
- [14] L. Mieville, D. Worledge, and T.H. Geballe, Transport across conducting ferromagnetic oxide/metal interfaces, *Appl. Phys. Lett.* **73**(12), 1736–1738 (1998), <http://dx.doi.org/10.1063/1.122261>.
- [15] L. Granja, L.E. Hueso, M. Quintero, P. Levy, and N.D. Mathur, Electrical transport properties of metal/ $\text{La}_{0.70}\text{Ca}_{0.30}\text{MnO}_3$ interfaces, *Physica B* **398**, 235–237 (2007), <http://dx.doi.org/10.1016/j.physb.2007.04.022>
- [16] B. Vengalis, J. Devenson, A.K. Oginskis, V. Lisauskas, F. Anisimovas, R. Butkute, and L. Dapkus, Optical and electrical properties of Nd-doped BiFeO_3 thin films and heterostructures, *Phys. Status Solidi C* **6**(12), 2746–2749 (2009), <http://dx.doi.org/10.1002/pssc.200982540>
- [17] L.F. Wang, X.L. Tan, P.F. Chen, B.W. Zhi, Z.G. Sun, Z. Huang, G.Y. Gao, and W.B. Wu, Anisotropic resistivities in anisotropic-strain-controlled phase-separated $\text{La}_{0.67}\text{Sr}_{0.33}\text{MnO}_3/\text{NdGaO}_3(100)$ films, *Appl. Phys. Lett.* **103**(7), 072407 (2013), <http://dx.doi.org/10.1063/1.4818636>
- [18] R.P. Borges, W. Guichard, J.G. Lunney, J.M.D. Coey, and F. Ott, Magnetic and electric “dead” layers in $(\text{La}_{0.7}\text{Sr}_{0.3})\text{MnO}_3$ thin films, *J. Appl. Phys.* **89**, 3868 (2001), <http://dx.doi.org/10.1063/1.1331658>
- [19] C.M. Xiong, J.R. Suna, and B.G. Shen, Dependence of magnetic anisotropy of the $\text{La}_{0.67}\text{Ca}_{0.33}\text{MnO}_3$ films on substrate and film thickness, *Solid State Commun.* **34**, 465–469 (2005), <http://dx.doi.org/10.1016/j.ssc.2005.02.020>
- [20] P. Zhang, On the spreading resistance of thin film contacts, *IEEE Trans. Electron Dev.* **59**(7), 1936–1940 (2012), <http://dx.doi.org/10.1109/TED.2012.2195317>

MAŽO PLOTO $\text{Ag}/\text{La}_{2/3}\text{Sr}_{1/3}\text{MnO}_3$ SANDŪRŲ ELEKTRINĖS IR MAGNETOVARŽOS SAVYBĖS

I. Černiukė^a, B. Vengalis^a, A. Steikūnienė^a, G. Grigaliūnaitė-Vonsevičienė^b, A.K. Oginskis^a

^a *Fizinių ir technologijos mokslų centras, Vilnius, Lietuva*

^b *Vilniaus Gedimino technikos universitetas, Vilnius, Lietuva*

Santrauka

Darbe tirtos susidariusios mažo ploto $\text{Ag}/\text{La}_{2/3}\text{Sr}_{1/3}\text{MnO}_3$ (Ag/LSMO) sandūros elektrinės ir magnetovaržos savybės. Šios sandūros buvo sudaromos mechaniškai prispaudžiant sulenktą Ag vielą ($\varnothing = 0,25$ mm) prie plono (LSMO) sluoksnio, užauginto magnetroninio dulkiniavimo būdu ant kristalinio $\text{MgO}(100)$ padėklo, esant 800 °C temperatūrai. Didžiausios tokių sandūrų magnetovaržos vertės, siekiančios 13 % (kai $\mu_0 H = 0,73$ T), buvo išmatuotos 295 K temperatūroje naudojant 3-jų elektrodų

būdą. Tyrimai parodė, kad darbe tyrinėtų mažo ploto Ag/LSMO sandūrų elektrinės ir magnetovaržos savybės lemia po elektrodų esantis ribotas medžiagos tūris, kuriame sutelktos srovės tankio linijos ir jį atitinkanti vadinamoji sutelkėjimo elektrinė varža. Papildoma didelės elektrinės varžos paviršinio sluoksnio įtaka buvo parodyta tiriant sandūras, sudarytas ant ilgą laiką ore išlaikytų LSMO sluoksnių paviršiaus, taip pat ant sluoksnio paviršiaus užgarinus ypač ploną ($d \sim 3\text{--}5$ nm) didelės elektrinės varžos BiFeO_3 junginio sluoksnį.